J Supercond Nov Magn (2012) 25:2481–2487
DOI 10.1007/s10948-012-1673-3

ORIGINAL PAPER

Physical Properties and Diffusion-Coefficient Calculation of Iron Diffused Bi-2223 System

O. Ozturk · E. Asikuzun · S. Kaya · M. Coskunyurek · G. Yildirim · M. Yilmazlar · C. Terzioglu

Received: 20 April 2012 / Accepted: 24 May 2012 / Published online: 9 June 2012

Abstract This study includes two parts: (I) investigation of the effect of different annealing time (10 h, 30 h, and 60 h) on physical, superconducting, and microstructural properties of Fe-diffused Bi-2223 superconductor ceramics prepared by the conventional solid-state reaction method with the aid of the X-ray diffraction (XRD), scanning electron microscopy (SEM), dc resistivity (ρ–T) and transport critical current density (J_c) measurements, and (II) determination of the diffusion coefficient and the activation energy of iron in the Bi-2223 system. In the former part, the zero-resistivity transition temperature (T_c), phase purity, volume fraction, hole-carrier concentration, lattice parameters, surface morphology, texturing, crystallinity, grain connectivity, grain size, and room temperature resistivity values of the bulk samples are found and compared with each other. The results obtained show that both the zero resistivity transition temperature (T_c) and transport critical current density (J_c) regularly enhance with the increment in the diffusion-annealing time. The maximum T_c of 107 ± 0.2 K and J_c of 50.0 A cm^{-2} are observed for the sample annealed at 830 °C for 60 h. As for the XRD investigations, according to the refinement of cell parameters done by considering the structural modulation, the enhancement in the diffusion-annealing is confirmed by both a decrease of the cell parameter a and an increase of the lattice parameter c of the samples, meaning that the greatest Bi-2223 phase fraction belongs to the sample annealed at 830 °C for 60 h. Moreover, SEM images display that the sample has the best crystallinity, grain connectivity, and largest grain size. Based on the results, the superconducting and microstructural properties improve with the increase in the diffusion-annealing time. In the latter part, Fe diffusion in the Bi-2223 system is examined in a range of 500–830 °C by the variation of the lattice parameters evaluated from the XRD patterns. The temperature dependence of the Fe diffusion coefficient is described by the Arrhenius relation $D = 4.27 \times 10^{-5} \exp(-1.27 \pm 0.10)$ eV/k$_B$T, and the related activation energy of the iron in the Bi-2223 system is found to be about 1.27 eV. The relatively low value of activation energy obtained illustrates that the migration of the Fe ions primarily proceeds through defects such as pore surfaces and grain boundaries in the polycrystalline structure, leading to the improvement of the microstructural and superconducting properties of the samples, supported by the results of part I. All in all, the aim of the present study is not only to analyze the role of diffusion-annealing time on superconducting and microstructural properties of Fe-diffused Bi-2223 superconductors, but also to find the diffusion coefficient and activation energy of Fe in the Bi-2223 system.

Keywords Fe-diffused Bi-2223 · Diffusion coefficient · XRD · SEM

O. Ozturk · E. Asikuzun (✉) · S. Kaya · M. Coskunyurek
Arts and Science Faculty, Department of Physics, Kastamonu University, 37100 Kastamonu, Turkey
e-mail: easikuzun@kastamonu.edu.tr

G. Yildirim · C. Terzioglu
Arts and Science Faculty, Department of Physics, Abant Izzet Baysal University, 14280 Bolu, Turkey

M. Yilmazlar
Faculty of Education, Sakarya University, 54300 Hendek, Sakarya, Turkey

1 Introduction

After the discovery of the high-temperature superconductors (HTS), several researches have been carried out to improve

the electrical, mechanical, microstructural, pinning mechanism, and superconducting properties of these superconductors by means of the addition, partial substitution, and diffusion technique [1–9]. Among the high-temperature superconductors, Bi-based superconductors are successfully used in practical applications such as fabrication of long-length wires and tapes [10]. The Bi–Sr–Ca–Cu–O (BSCCO) system has three superconducting phases in terms of its chemical compositions, the Bi-2201 phase ($Bi_2Sr_2Cu_1O_x$, $T_c \approx 20$ K), Bi-2212 phase ($Bi_2Sr_2Ca_1Cu_2O_x$, $T_c \approx 85$ K), and Bi-2223 phase ($Bi_2Sr_2Ca_2Cu_3O_x$, $T_c \approx 110$ K) [11–14]. In these series, the (Bi, Pb)-2223 phase is the most attractive owing to the highest critical temperature (T_c) of about 110 K. However, their applications in magnetic fields and high temperatures are restricted because of the structural layer, very low charge carrier density, strong anisotropic properties, extremely short coherence length, and large penetration depth and brittleness nature. Hence, many methods have been studied for improvement of their superconducting, mechanical, structural, and flux pinning properties to make them suitable for high temperature and magnetic field applications [15–17]. In our previous works, we have studied the effects of iron diffusion on the superconducting and mechanical properties of Bi-2223 systems [18–20]. We have observed that the mechanical properties of the samples were load dependent. The load-independent Vickers hardness (H_0), Young's modulus (E), yield strength (Y), and fracture toughness (K_{IC}) values of the samples prepared were found to enhance with the increase in the Fe diffusion and annealing time. Based on these results, the iron diffusion improves the mechanical properties of the Bi-2223 ceramics.

As is well known, the diffusion rate of impurities described as the diffusion coefficient is related to how fast the impurity atoms act in the crystal. Therefore, the diffusion coefficient of iron could be useful to understand the doping mechanism and changes in the microstructural and superconducting properties of BSCCO systems. To our knowledge, there is no detailed work on the calculation of iron diffusion-coefficient in the Bi-2223 system in the literature. In our previous study, we have investigated the effect of the annealing time on the microstructural, mechanical, and superconducting properties of Au-diffused Bi-2223 samples and also calculated the diffusion-coefficient of Au in the Bi-2223 system [21–23].

In the present work, not only the effect of the annealing time on microstructural and superconducting properties of Fe-diffused Bi-2223 superconducting ceramics is investigated by performing XRD, SEM, dc resistivity, and transport critical current density measurements, but the diffusion coefficient and the activation energy of iron in the Bi-2223 system are also examined with the aid of the successive removal of thin layers and measurement of the cell parameter c for the first time. The results obtained show that the Fe diffusion enhances the microstructural and superconducting properties of the samples studied as a result of the improvement of crystallinity and connectivity between grains (inferred from the first part of the paper). Moreover, the second part of the paper displays that the temperature dependence of the Fe diffusion coefficient described by the Arrhenius relation is found to be $D = 4.27 \times 10^{-5} \exp(-1.27 \pm 0.10)$ eV/k_BT, which will be explained in detail in results and discussion part.

2 Experimental Details

Superconducting $Bi_{1.8}Pb_{0.35}Sr_{1.9}Ca_{2.1}Cu_3O_y$ ceramics are elaborated in air by the conventional solid-state reaction method using high-purity starting powders of Bi_2O_3 (99.99 %), PbO (99.9+ %), $SrCO_3$ (99.9+ %), $CaCO_3$ (99+ %), and CuO (99+ %) in the cation ratio of Bi:Pb:Sr:Ca:Cu = 1.8:0.35:1.9:2.1:3. These oxides and carbonates are weighed in stoichiometric proportion and mixed in a grinding machine for 24 h to obtain a homogeneous mixture. After milling process, the resultant powder is calcined in air at different temperature such as 700, 750, and 800 °C for 24 h in a tube furnace (PROTHERM Model PTF 12/75/200) at 5 °C/min heating rate. Then, the samples are cooled to room temperature and reground. The powder calcined is pressed into pellets with the dimension of $10 \times 4 \times 2$ mm^3 at 300 MPa. The sintering process of the pellets obtained is conducted in air at 830 °C for 48 h. The heating and cooling rate of the furnace are chosen to be 10 and 3 °C min^{-1}, respectively. Thus, the Bi-2223 samples are ready for the evaporation process. The Fe evaporation on one face of the samples is carried out using an AUTO 306 Vacuum Coater (EDWARDS). After evaporation process, it is controlled that the Fe attached to the Bi-2223 superconducting ceramics by visual inspection and the mechanical damage method via a razor blade. Then, the Fe evaporated Bi-2223 superconductors are sintered at 830 °C for 10 h, 30 h, and 60 h and herein after denoted as F1, F2, and F3, respectively. Similarly, an undoped sample sintered under the same conditions will be shown as F0.

The electrical property of the samples is examined by dc resistivity versus temperature measurements using 5 mA dc current through the samples in the temperature range from 90 to 130 K. Both voltage and current contacts are made with silver glue contact for the minimization of resistance. A Keithley 220 programmable current source and a Keithley 2182A nano-voltmeter system are used for the conventional four-probe measurements. Likewise, the transport critical current measurement of the samples in self-field is performed at 77 K in zero field using four-probe method. A programmable temperature controller (Lakeshore 340) is

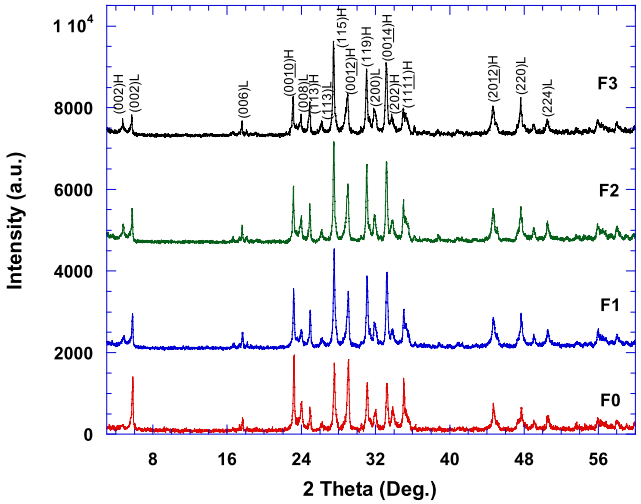

Fig. 1 XRD patterns of the samples annealed at 830 °C for 10 h (F0) and (F1), 30 h (F2), and 60 h (F3)

used for the accurate monitoring of the temperature with a stability and accuracy of ±0.01 K. The current applied parallel to the direction of pressed surface is ramped at a constant rate (10 mA/s) for the entire sample. The critical current (I_c) values of the samples are described with the criterion of 1 μV/cm. The J_c values are computed from the relationship between I_c and the total cross-sectional area [24].

The surface morphology, crystallinity, and grain connectivity of the samples prepared in this work are studied by means of a Philips XL30 SFEG Scanning Electron Microscope (SEM) with an accelerating voltage of 15 kV in the secondary electron image mode. Moreover, the crystalline quality, grain orientations, and phase analysis of the pure and Fe-doped samples are determined by X-ray diffractometer (XRD) analysis at room temperature (Rigaku D/Max-IIIC diffractometer), using Cu$K\alpha$ radiation with wavelength of 1.5418 Å and incident angles in the range of 2θ between 5° and 60° at a scan speed of 3°/min and a step increment of 0.02°. The X-ray tube voltage and the current are adjusted to 36 kV and 26 mA, respectively. The lattice parameters of the samples are evaluated from the XRD peaks with the accuracy of ±0.001 Å.

The relative volume fractions of the Bi-2223 and Bi-2212 phases are estimated from the XRD patterns using the following expressions [25, 26]:

$$f_{(2223)} = \frac{\sum I_{H(hkl)}}{\sum I_{H(hkl)} + \sum I_{L(hkl)}}, \tag{1}$$

$$f_{(2212)} = \frac{\sum I_{L(hkl)}}{\sum I_{H(hkl)} + \sum I_{L(hkl)}}, \tag{2}$$

where $I_{H(hkl)}$ and $I_{L(hkl)}$ are the intensities of the (hkl) diffraction lines for Bi-2223 and Bi-2212 phases, respectively (Fig. 1).

For part II of the paper, the samples prepared are annealed at different temperature such as 500, 600, 700, 800, and 830 °C for 10 h, and the diffusion coefficient and activation energy of Fe are determined using the successive removal of thin layers and measurement of the cell parameter c. According to the variation of the cell parameters determined, it is observed that the substitution of matrix atom by impurity atom with a different radius leads to a deformation near the impurity atom [27], resulting in the change of lattice parameters in the specimen. The deformation (ε) in the crystalline lattice region at point x due to the radii of impurity and matrix atoms is shown by

$$\varepsilon(x) = \big[c(x) - c_0\big]/c_0, \tag{3}$$

where $c(x)$ and c_0 are the lattice parameters in the deformed and nondeformed region of the samples, respectively. The concentration of impurity atoms, $N(x)$, is also given as the following relation:

$$\varepsilon(x) = \beta N(x), \tag{4}$$

where β denotes the expansion coefficient of the lattice given by the equation

$$\beta = \frac{1}{3N_\ell}\left[1 - \left(\frac{r_i}{r_0}\right)^3\right], \tag{5}$$

where r_i and r_0 are the radii of the impurity and the matrix atoms, respectively, and N_ℓ presents the concentration of the matrix atoms. Hence, the measurement of the distribution of deformation ($\varepsilon(x) = \Delta c/c_0$) over the thickness gives the information about the concentration profile of the diffusing impurity in the Fe-diffused samples.

Additionally, it is supposed that the conditions of impurity diffusion from a constant source into semi-infinite solid are fulfilled by means of the following equation [27]:

$$N(x,t) = N_0\big[1 - erf(x/2\sqrt{Dt})\big], \tag{6}$$

where $erf[x/2(Dt)^{1/2}]$ illustrates the error function with argument $y = x/2(Dt)^{1/2}$,

$$erf(y) = \frac{2}{\sqrt{\pi}}\int_0^y \exp\big(-y^2\big). \tag{7}$$

Here $N_0 = N(0,t)$ denotes the constant concentration on the surface of the sample, and $N(x,t)$ is the impurity concentration at the distance x. Besides, D is the diffusion coefficient when t presents the diffusion annealing time.

3 Result and Discussions

3.1 XRD Characterization

The XRD patterns from the surfaces of the F0, F1, F2, and F3 samples are depicted in Fig. 1. The (Bi, Pb)-2223 peaks

Table 1 Critical temperature T_c, lattice parameters a and c, transport critical current density J_c, hole-carrier concentration, volume fraction, and grain size of the samples prepared

Samples	T_c^{offset} (K)	c (Å)	a (Å)	J_c^{trans} (A/cm^2)	Hole concentration (p)	Volume fraction (%)		Grain size (nm)
						2212	2223	
F0	100.0 ± 0.2	36.96	5.431	32.5	0.127	34.00	66.00	76.24
F1	106.0 ± 0.2	37.00	5.391	50.0	0.139	25.70	74.30	86.88
F2	106.5 ± 0.2	37.10	5.380	56.2	0.140	18.30	81.70	87.78
F3	107.0 ± 0.2	37.16	5.373	65.0	0.141	11.80	88.90	88.09

are shown by H (hkl) Miller indices, while the peaks of (Bi, Pb)-2212 phase are presented by L (hkl) Miller indices given in the diagrams. All the samples prepared exhibit the polycrystalline superconducting phase. It is visible from the figure that the F3 sample points up the highest peak intensities belonging to Bi-2223 phase, whereas the Bi-2212 phase is denser than other phase in the F0 sample. According to the result, the formation of Bi-2223 phase increases with the enhancement in the diffusion-annealing time. Furthermore, the relative volume fractions of Bi-2223 and Bi-2212 phases calculated by using expressions (1) and (2) are listed in Table 1. As seen from the table, the volume fraction values of Bi-2223 phase increases, while that of Bi-2212 phase decreases with the increment in the diffusion-annealing time. Moreover, the lattice parameters a and c are computed using the least square method through d value and hkl planes for tetragonal unit cell structure [28–32]. Their variations as a function of the annealing time are also tabulated in Table 1. It is visible from the table that a systematic contraction in the a-axis length is observed while a regular expansion in the c-axis length is obtained with the increase [33] in the diffusion-annealing time. As received the cell parameter a is controlled by the length of in-plane Cu–O bond [34]. The length may be expanded or contracted with the change of the electrons into antibonding orbital. In our system, it seems a contradiction in the bond length, leading to a reduction of the lattice parameter a, and an enhancement in the cell parameter c. According to these results, it might be interpreted that the (Bi, Pb)-2223 phase increases while the (Bi, Pb)-2212 phase starts to decrease with the increase of the diffusion-annealing time; nevertheless, Fig. 1 confirms that the (Bi, Pb)-2223 phase is dominant for all the samples studied.

The grain size of the samples are determined by using the following equation:

$$D = 0.94\lambda/\beta \cos\theta_\beta. \tag{8}$$

The calculated grain size values of all the samples are depicted in Table 1. As seen from the table, the grain size values increase from 7.624 to 8.809 with the increment in the diffusion-annealing time, revealing that the largest grain size and best crystallinity are obtained for the F3 sample (Table 1).

3.2 SEM Analysis

The microstructural characterization of the samples produced is analyzed by Scanning Electron Microscopy (SEM) method for the determination of the grain size and the possible precipitation at the grain boundaries. Figures 2a and 2b show the SEM micrographs taken in the secondary electron image mode of the fractured surface of the F0 and F3 samples. As is seen from the figure, the surface morphology of the samples depends strongly on the diffusion-annealing time. The microstructure of undoped sample shows flake-type grains (the basic characteristics of (Bi, Pb)-2212 phase formation [35]) oriented randomly and poorly connected. On the other hand, the texturing, crystallinity, and layered grain growth of the F3 sample are observed to be better compared to the F0 sample, and the surface of the F3 sample is found to be more uniform with better alignment of grains. Additionally, SEM image of the F3 sample gives a broader grain size distribution in comparison with the other one. Based on the results of the SEM investigations, the F3 sample has the larger average grain size and better crystallinity and grain connectivity. These observations are in excellent agreement with the XRD examinations.

3.3 Electrical Measurements

Electrical resistivity measurements are performed by standard four-probe dc technique in the temperature range between 90 and 130 K. Figure 3 shows the normalized electrical resistivity as a function of temperature for the F0, F1, F2, and F3 samples. It is visible form the figure that all the samples show metallic behavior above the T_c value, and the resistivity at room temperature regularly decreases with the increment in the diffusion-annealing time as a result of the increase in the grains [36]. Further, the zero-resistivity transition temperatures ($R = 0$ Ω) deduced from the dc resistivity measurements of the F0, F1, F2, and F3 samples are found to be about 100 ± 0.2 K, 106 ± 0.2 K, 106.5 ± 0.2 K, and 107 ± 0.2 K, respectively. According to the results,

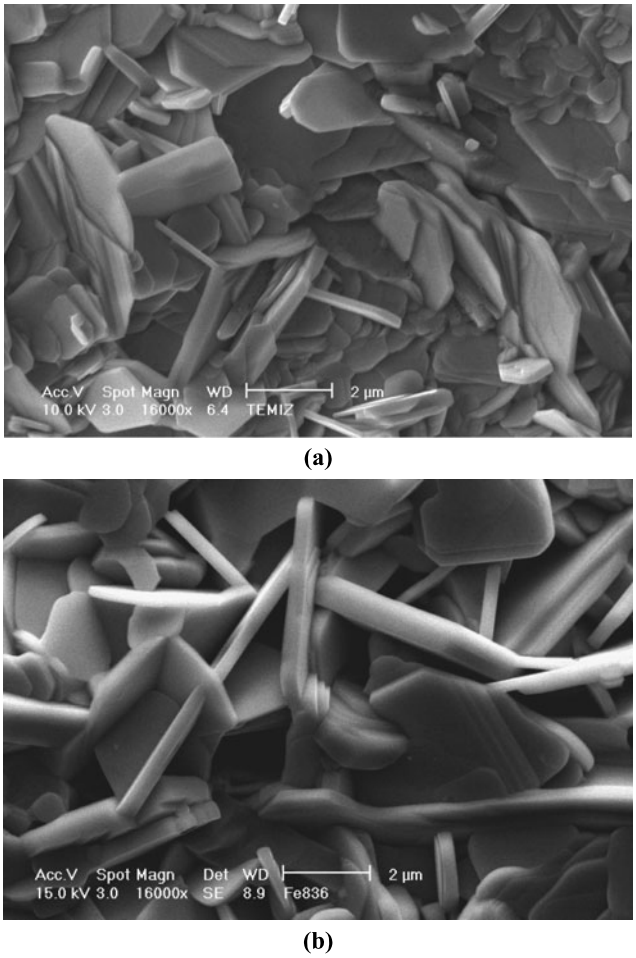

Fig. 2 SEM micrographs of the F0 (**a**) and F3 (**b**) samples

the T_c value is noticed to enhance with the increase of the diffusion-annealing time, attributed to the increment in the relative percentage of (Bi, Pb)-2223 phase formation [37, 38], the optimization of the hole concentration and possible changes in the lattice vibration of Bi(Pb)–Sr–Ca–Cu–O [39, 40]. It is also possible that the resistive nature of the grain boundaries is modified owing to the accumulation of iron atoms at the grain boundaries. Moreover, it is interesting to note that the variation of ΔT_c ($T_c^{\text{onset}} - T_c^{\text{offset}}$) reduces dramatically as the annealing time increase up to 60 h. The variation is observed to be about 8 K for the F0 sample when the ΔT_c is obtained to be about 4 K for the F3 sample. As for the broadening of the resistive transition, with the enhancement in the diffusion-annealing time the broadening region systematically reduces as a result of the modifying effect of the iron doping on the grain boundaries [36]. Besides, Fig. 3 demonstrates that the transition curve of the F0 sample exhibits a double step transition due to the weak links between the superconducting grains in this sample [36], leading to the dominancy of the low-T_c phase, which is also supported by the XRD measurement.

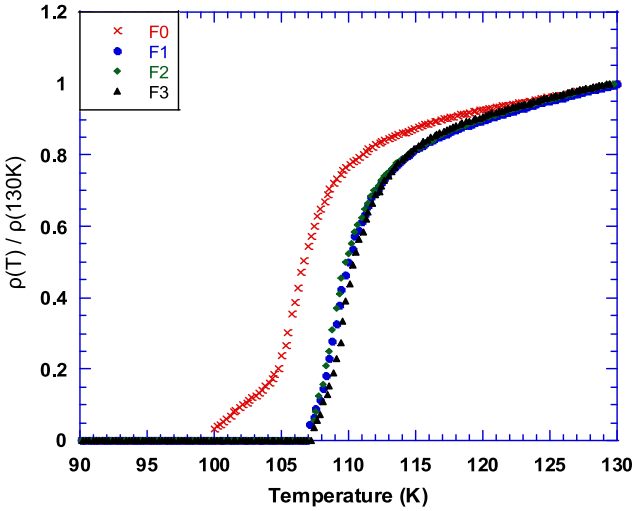

Fig. 3 Electrical resistivity-temperature plots of pure (F0) sample annealed at 830 °C for 10 h and Fe-diffused samples sintered at 830 °C for 10 h (F1), 30 h (F2), and 60 h (F3)

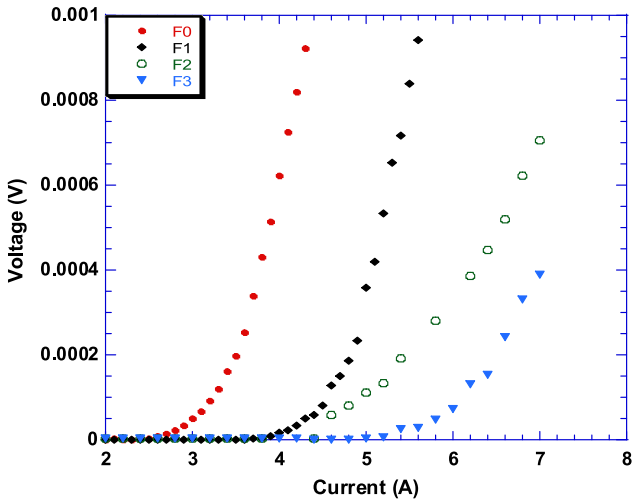

Fig. 4 Current–voltage characteristics of the F0, F1, F2, and F3 samples

The transport critical current of the samples in self-field are measured by home-made system at 77 K in zero field using four-probe method. I–V curves measured are shown in Fig. 4. The critical current (I_c) values of the samples are defined with the criterion of 1 µV/cm. Critical current densities (J_c) of the samples produced are calculated from the I_c and the total cross-sectional area. The J_c values obtained are shown in Table 1. It is apparent from the table that the J_c values increase from 32.5 to 65.0 A/cm^2 with the enhancement in the diffusion-annealing time owing to the improvement of crystallinity and connectivity between grains [41], indicating that the increment in the annealing time has a positive effect on the J_c values of the samples.

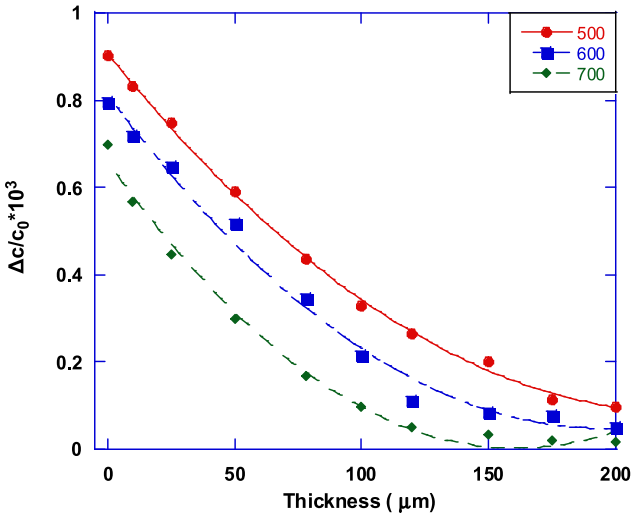

Fig. 5 Distribution of deformation $\Delta c/c$ versus the thickness of diffused Bi-2223 samples at 800 °C for 10 h (full curve is calculated according to (6))

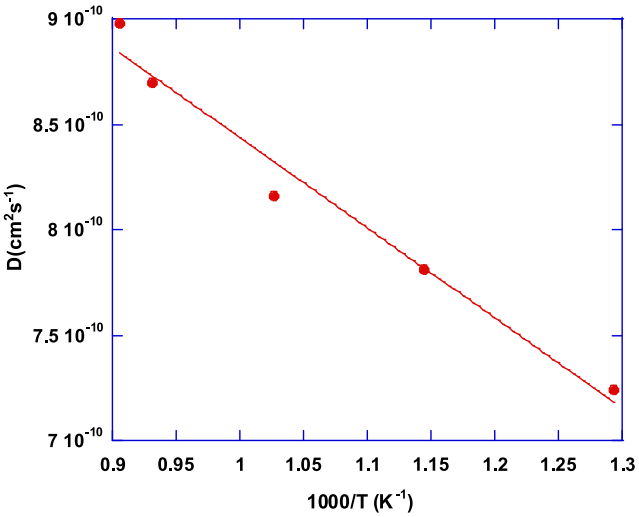

Fig. 6 Temperature dependence of Fe diffusion coefficient in the Bi-2223 superconductors

The hole-carrier concentration (P) is calculated by using the following relation [42]:

$$T_c/T_c^{\max} = 1 - 82.6(P - 0.16)^2, \tag{9}$$

where $T_c^{\max}$ is taken as 110 K for Bi-2223 system, and the T_c values of the samples are deduced from Fig. 3. The hole-carrier concentrations calculated are tabulated in Table 1. It is observed that the P value regularly increases from 0.127 to 0.141 with ascending the diffusion-annealing temperature due to the optimization of the hole density, indicating the possible changes in the lattice vibration of the system.

There are several methods to determine the diffusion parameter in a polycrystalline high-T_c. In literature, successive removal of thin layers and (1) the measurement of the samples resistivity, (2) the measurement of lattice parameters from XRD patterns, (3) the radio tracer, and (4) the EDXRF technique are the most common four methods. The second method (successive removal of thin layers and measurement of the lattice parameter c at room temperature) is used to find the diffusion coefficient of Fe in the Bi-2223 system in the present work. Figure 5 shows the variation of lattice parameter $\Delta c/c_o$ (c_o denotes the lattice parameter of the undoped sample) as a function of thickness of the samples exposed to the iron diffusion at different annealing temperature such as 500, 600, and 700 °C for 60 h. For the Fe-diffused sample annealed at 800 °C for 60 h, the experimental data of Fig. 5 fits well with the theoretical curve obtained from (6) for $D = 8.70 \times 10^{-10}$ cm^2 s^{-1}. The same fitting method is used for the samples annealed at 500, 600, 700, and 830 °C, and the diffusion coefficients for the other samples are determined. According to the result, the diffusion coefficients obtained are found to increase as the annealing temperature enhances, presenting that the diffusion at lower temperatures is much less significant than the higher ones. Figure 6 gives the mean values of the diffusion coefficients of Fe in the Bi-2223 superconductor material as a function of annealing temperature. It is obvious from the figure that the Fe diffusion coefficient in the Bi-2223 system in the temperature range from 500 to 830 °C increases with respect to the Arrhenius relation,

$$D = 4.27 \times 10^{-10} \exp\{(-1.27 \pm 0.10)\ \text{eV}/k_B T\}. \tag{10}$$

The relatively low value of activation energy found to be 1.27 eV of Fe in the Bi-2223 system may testify that the migration of the iron primarily proceeds through defects in the polycrystalline sample (pore surfaces, grain boundaries, etc.), leading to the improvement of the superconducting and microstructural properties of the samples prepared in this work. Similar results were reported for Fe diffusion in YBaCuO ceramics [43].

4 Conclusions

In this work, it is analyzed that not only how the different annealing time (10 h, 30 h, and 60 h) affects the microstructural, physical, and superconducting properties of Fe-diffused Bi-2223 superconductor ceramics by means of the SEM, XRD, ρ–T, and I–V measurements, but also the diffusion coefficient and the activation energy of iron in the Bi-2223 system are investigated using the change in the cell parameters deduced from the XRD patterns. It is observed that the microstructural and superconducting properties improve with the increase in the diffusion-annealing time. The ρ–T and I–V measurements of the samples show that with ascending the annealing time up to 60 h, the T_c

and J_c values enhance from 100 ± 0.2 K to 107 ± 0.2 K and 32.5 A cm^{-2} to 50.0 A cm^{-2}, respectively. Likewise, hole-carrier concentration increases from 0.127 to 0.141. Furthermore, the XRD investigations give that the lattice parameter a reduces, while c parameter enhances with the increment in the diffusion-annealing time. The maximum Bi-2223 phase fraction and grain size values inferred from the XRD pattern are observed for the sample annealed at 830 °C for 60 h. Similarly, the SEM images reveal that the largest average crystallite size and the best surface morphology and grain connectivity are observed for that sample. In addition, the change in the c parameters is used to determine the diffusion coefficient and activation energy of Fe in the Bi-2223 system. According to the calculations, the coefficient systematically increases from 7.24×10^{-10} to 8.78×10^{-10} with the enhancement of the diffusion-annealing time. In other words, the minimum value is obtained for the undiffused sample (F0), whereas the maximum one is attributed to the F3 sample. The corresponding activation energy is determined to be about 1.27 eV. The low value of the activation energy reveals that Fe diffusion proceeds through defects in the ceramic samples, resulting in the improvement of the microstructural and superconducting properties of the bulk samples prepared in this work.

References

1. Li, Y., Kavıraj, S., Berenov, A., Perkıns, G.K., Drıscoll, J., Caplın, A.D., Cao, G.H., Ma, Q.Z., Wang, B., Wei, L., Zhao, Z.X.: Physica C **355**, 51 (2001)
2. Dzhafarow, T.D., Altunbaş, M., Küçükömeroğlu, T., Nezir, S.: Solid State Commun. **99**, 839 (1996)
3. Terzioglu, C., Yilmazlar, M., Ozturk, O., Yanmaz, E.: Physica C **423**, 119 (2005)
4. Dzhafarow, T.D., Cömert, H., Altunbaş, M., Alver, U., Küçükömeroğlu, T., Kopya, A.: J. Alloys Compd. **221**, 264 (1995)
5. Kishore, K.N., Muralidhar, M., Babu, V.H.: Physica C **204**, 299 (1993)
6. Dzhafarow, T.D., Yilmazlar, M.: Physica C **292**, 140 (1997)
7. Ilyushechkin, A.Y., Yamashita, T., Boskovic, L., Mackinnon, I.D.R.: Supercond. Sci. Technol. **17**, 1201 (2004)
8. Biju, A., Aloysius, P., Sayamaprasad, U.: Sci. Technol. **18**, 1854 (2005)
9. Prabıtha, V.G., Biju, A., Abhılashkumar, R.G., Sarun, P.M., Aloysıus, R.P., Syamaprasad, U.: Physica C **433**, 28 (2005)
10. Maeda, H., Tanaka, Y., Fukutomi, M., Asano, T.: Jpn. J. Appl. Phys. A **27**(2), L209 (1988)
11. Gao, L., Huang, J.Z., Meng, L.R., Hor, H.P., Bechtold, J., Sun, Y.Y., Chu, W.C., Chen, Z.Z., Herman, M.A.: Bulk Nature **332**, 623 (1998)
12. Chu, W.C., Bechtold, J., Gao, L., Hor, H.P., Huang, J.Z., Meng, L.R., Sun, Y.Y., Wang, Y.Q., Zue, Y.Y.: Phys. Rev. Lett. **60**, 941 (1988)
13. Tallon, L.J., Buckley, G.R., Gilbert, W.P., Presland, R.M., Brown, M.W.I., Bowder, E.M., Christan, A.L., Gafull, R.: Nature **333**, 153 (1988)
14. Abbasi, H., Taghipour, J., Sedghi, H.: J. Alloys Compd. **482**, 552–555 (2009)
15. Sarun, P.M., Vinu, S., Shabna, R., Biju, A., Syamaprasad, U.: Mater. Res. Bull. **44**, 1017 (2009)
16. Yildirim, G., Bal, S., Varilci, A.: J. Supercond. Nov. Magn. (2012). doi:10.1007/s10948-012-1496-2
17. Yildirim, G., Bal, S., Varilci, A.: J. Supercond. Nov. Magn. (2012). doi:10.1007/s10948-012-1497-1
18. Ozturk, O., Cetinkara, H.A., Asikuzun, E., Akdogan, M., Yilmazlar, M., Terzioglu, C.: J. Mater. Sci., Mater. Electron. **22**, 1501–1508 (2011)
19. Ozturk, O.: J. Mater. Sci., Mater. Electron. (2011). doi:10.1007/s10854-011-0580-x
20. Dzhafarov, T.D.: Phys. Status Solidi A **158**, 335 (1996)
21. Yilmazlar, M., Ozturk, O., Gorur, O., Belenli, I., Terzioglu, C.: Supercond. Sci. Technol. **20**, 365 (2007)
22. Ozturk, O., Terzioglu, C., Belenli, I.: J. Supercond. Nov. Magn. **24**, 381–390 (2011)
23. Ozturk, O., Kucukomeroglu, T., Terzioglu, C.: J. Condens. Matter **19**, 346205 (2007)
24. Yildirim, G., Akdogan, M., Altintas, S.P., Erdem, M., Terzioglu Varilci A, C.: Terzioglu Varilci A, C.: Physica B **406**, 1853–1857 (2011)
25. Chiu, C.W., Meng, R.L., Gao, L., Huang, Z.J., Chen, F., Xue, Y.Y.: Nature **365**, 323 (1993)
26. Halim, S.A., Khawaldeh, S.A., Mohammed, S.B., Azhan, H.: Mater. Chem. Phys. **61**, 251 (1999)
27. Abdullaev, G.B., Dzhafarov, T.D.: Atomic Diffusion in Semiconductor Structures. Harwood, New York (1987)
28. Vinu, S., Sarun, P.M., Biju, A., Shabna, R., Guruswamy, P., Syamaprasad, U.: Supercond. Sci. Technol. **21**, 045001 (2008)
29. Sarun, P.M., Vinu, S., Shabna, R., Biju, A., Syamaprasad, U.: J. Alloys Compd. **472**, 13 (2009)
30. Vinu, S., Sarun, P.M., Shabna, R., Biju, A., Syamaprasad, U.: Mater. Lett. **62**, 4421 (2008)
31. Shabna, R., Sarun, P.M., Vinu, S., Biju, A., Syamaprasad, U.: J. Alloys Compd. **493**, 11 (2010)
32. Sarun, P.M., Vinu, S., Shabna, R., Biju, A., Syamaprasad, U.: Mater. Lett. **62**, 2725 (2008)
33. Biju, A., Sarun, P.M., Aloysius, R.P., Syamaprasad, U.: J. Alloys Compd. **454**, 46 (2008)
34. Sarun, P.M., Vinu, S., Shabna, R., Biju, A., Syamaprasad, U.: Mater. Res. Bull. **44**, 1017 (2009)
35. Khalil, S.M.: J. Phys. Chem. Solids **62**, 457–466 (2001)
36. Kameli, P., Salamati, H., Eslami, M.: Solid State Commun. **137**, 30–35 (2006)
37. Yildirim, G., Yucel, E., Bal, S., Dogruer, M., Varilci, A., Akdogan, M., Terzioglu, C., Zalaoglu, Y.: J. Supercond. Nov. Magn. **25**, 231–237 (2012)
38. Yildirim, G., Bal, S., Yucel, E., Dogruer, M., Akdogan, M., Varilci, A., Terzioglu, C.: J. Supercond. Nov. Magn. **25**, 381–390 (2012)
39. Nursoy, M., Yilmazlar, M., Terzioglu, C., Belenli, I.: J. Alloys Compd. **4591–4592**, 399 (2008)
40. Ling, H.C., Yan, M.F.: J. Appl. Phys. **64**, 1307 (1988)
41. Ozturk, O., Yegen, D., Yilmazlar, M., Varilci, A., Terzioglu, C.: Physica C **451**, 113–117 (2007)
42. Persland, M.R., Tallon, J.L., Buckley, R.G., Liu, R.S., Flower, N.E.: Physica C **176**, 95 (1991)
43. Dzhafarov, T.D., Altunbaş, M., Varilci, A., Küçükömeroğlu, T.: Mater. Lett. **25**, 81 (1995)